

## Appendix B

### Cross-dimensional Rethermalization Supplement

*Wherein the author leaves a record of various details and equations whose complexity renders them a distraction elsewhere.*

#### B.1 Thermal Averages with Different Anisotropies for Each Species

Although our theory described in Ref. [66] assumes separable Gaussian distributions for each species in each direction, the center-of-mass (CM) and relative velocities are generally correlated if the energy anisotropy is not the same between species. To see this, note that

$$\frac{1}{2} \left( \frac{m_1 v_{1i}^2}{E_{1i}} + \frac{m_2 v_{2i}^2}{E_{2i}} \right) = \frac{1}{2} \left( \frac{M V_{\text{CM}i}^2}{\epsilon_{\text{CM}i}} + \frac{\mu v_{\text{rel}i}^2}{\epsilon_{\text{rel}i}} \right) - \mu \delta_i V_{\text{CM}i} v_{\text{rel}i} \quad , \quad (\text{B.1})$$

where  $E_{\sigma i}$  is the mean energy for species  $\sigma$  in the  $i^{\text{th}}$  direction, and we have defined

$$\begin{aligned} \epsilon_{\text{CM}i} &= (m_1 + m_2) \frac{E_{1i} E_{2i}}{m_2 E_{1i} + m_1 E_{2i}} \\ \epsilon_{\text{rel}i} &= \frac{m_2 E_{1i} + m_1 E_{2i}}{m_1 + m_2} \\ \delta_i &= \frac{E_{1i} - E_{2i}}{E_{1i} E_{2i}} \quad . \end{aligned} \quad (\text{B.2})$$

Although the energy anisotropy is the same for each species at the beginning and end of the experiment ( $\Omega$  and 1, respectively), the fact that  $\alpha$  and  $\beta$  are generally different means that the two species will have different anisotropies at intermediate times.

With the definitions above, and using the distribution function  $\exp(-H/k_B T)$ , one can calculate the following averages:

$$\begin{aligned}
\langle v_{\text{rel}} \rangle &= \sqrt{\frac{2 E_{\text{rel}z}}{\pi \mu}} [1 + \Omega_{\text{rel}} Q(\Omega_{\text{rel}})] \\
\langle v_{\text{rel}i}^2 \rangle &= \frac{E_{1i}}{m_1} + \frac{E_{2i}}{m_2} \\
\langle V_{\text{CM}i} v_{\text{rel}i} \rangle &= \frac{(E_{1i} - E_{2i}) E_{\text{rel}i}}{m_2 E_{1i} + m_1 E_{2i}} \\
\langle v_{\text{rel}} v_{\text{rel}z}^2 \rangle &= \frac{1}{\sqrt{2\pi}} \left( \frac{E_{\text{rel}z}}{\mu} \right)^{3/2} \frac{\Omega_{\text{rel}}}{\Omega_{\text{rel}} - 1} [3 \Omega_{\text{rel}} - 2 + (3 \Omega_{\text{rel}} - 4) \Omega_{\text{rel}} Q(\Omega_{\text{rel}})] \\
\langle v_{\text{rel}} v_{\text{rel}z}^2 \rangle &= \sqrt{\frac{2}{\pi}} \left( \frac{E_{\text{rel}z}}{\mu} \right)^{3/2} \frac{1}{\Omega_{\text{rel}} - 1} [\Omega_{\text{rel}} - 2 + \Omega_{\text{rel}}^2 Q(\Omega_{\text{rel}})] \\
\langle v_{\text{rel}} V_{\text{CM}i} v_{\text{rel}i} \rangle &= \left( \frac{m_1 m_2}{m_1 + m_2} \right) \frac{E_{1i} - E_{2i}}{m_2 E_{1i} + m_1 E_{2i}} \langle v_{\text{rel}} v_{\text{rel}i}^2 \rangle \quad , \quad (\text{B.3})
\end{aligned}$$

where we have introduced the definitions

$$\begin{aligned}
E_{\text{rel}i} &= \frac{m_2 E_{1i} + m_1 E_{2i}}{m_1 + m_2} \\
\Omega_{\text{rel}} &= \frac{E_{\text{rel}x}}{E_{\text{rel}z}} \\
Q(x) &= \begin{cases} \frac{\tanh^{-1} \sqrt{1-x}}{\sqrt{1-x}} & , \quad x < 1 \\ 1 & , \quad x = 1 \\ \frac{\tan^{-1} \sqrt{1-x}}{\sqrt{1-x}} & , \quad x > 1 \end{cases} \quad . \quad (\text{B.4})
\end{aligned}$$

We are now in a position to consider ratios of the type

$$\frac{\langle v_{\text{rel}} v_{\text{rel}z}^2 \rangle}{\langle v_{\text{rel}} \rangle \langle v_{\text{rel}z}^2 \rangle} \quad , \quad (\text{B.5})$$

which we claimed in Ref. [66] are roughly equal to 4/3 for reasonable anisotropies. As an example of a “reasonable” anisotropy, we take  $\Omega = 1.64$ , which we used in the CDR measurements and many of the MC simulations. Figure B.1 shows the ratio in Eq.(B.5) as a function of  $m_1/m_2$  for varying anisotropies  $\Omega_1$  and  $\Omega_2$ . In the “worst-case” scenario, where one species maintains  $\Omega = 1.64$  and the

other is isotropic, this ratio lies between 1.333 and 1.375 for any choice of masses, corresponding to only a 3% variation. In fact one can show more generally that this ratio is always between 1 and  $3/2$ .

Although it is not immediately evident from Eq.(B.3), one can additionally show that the averages of interest to our theoretical treatment (see Eq.(6) and following in Ref. [66]) are related by

$$\begin{aligned} \frac{\langle v_{\text{rel}} v_{\text{reli}}^2 \rangle}{\langle v_{\text{rel}} \rangle \langle v_{\text{reli}}^2 \rangle} &= \frac{\langle v_{\text{rel}} V_{\text{CM}i} v_{\text{reli}} \rangle}{\langle v_{\text{rel}} \rangle \langle V_{\text{CM}i} v_{\text{reli}} \rangle} \\ \frac{\langle v_{\text{rel}} v_{\text{rel}x}^2 \rangle}{\langle v_{\text{rel}} \rangle \langle v_{\text{rel}x}^2 \rangle} - \frac{4}{3} &= \frac{4}{3} - \frac{\langle v_{\text{rel}} v_{\text{rel}z}^2 \rangle}{\langle v_{\text{rel}} \rangle \langle v_{\text{rel}z}^2 \rangle} . \end{aligned} \quad (\text{B.6})$$

## B.2 Analytic Best Fit to Exponential Decay

In Ref. [66] we determined an upper limit  $\beta_u$  for the constant of proportionality  $\beta$ . We saw that the fermion relaxation, described by Eq.(8) in that work, does not generally correspond to pure exponential decay. In Fig. B.2 we compare solutions for the relaxation for light and heavy fermions, neglecting the effects of boson-boson collisions (*i.e.*, assuming  $\gamma = 0$  in the language of Ref. [66]). The light fermions begin to relax quickly, and then are held up by the residual anisotropy of the bosons. In contrast the heavy fermions relax slowly at first, and then somewhat more quickly as the energy of the bosons becomes more isotropic. In other words, for heavy fermions the small- $\tau$  behavior gives an estimate for  $\beta_u$  that reliably bounds  $\beta$  from above, but for light fermions something more robust is needed.

To determine the best approximation to pure exponential decay, we analytically minimize the integrated squared error

$$\text{err}^2 = \int_0^\infty d\tau \left[ \chi_1(\tau) - \exp\left(-\frac{\tau}{\beta_u}\right) \right]^2 \quad (\text{B.7})$$

with respect to the parameter  $\beta$ . Minimization of the error requires  $\partial/\partial\beta_u = 0$ ,

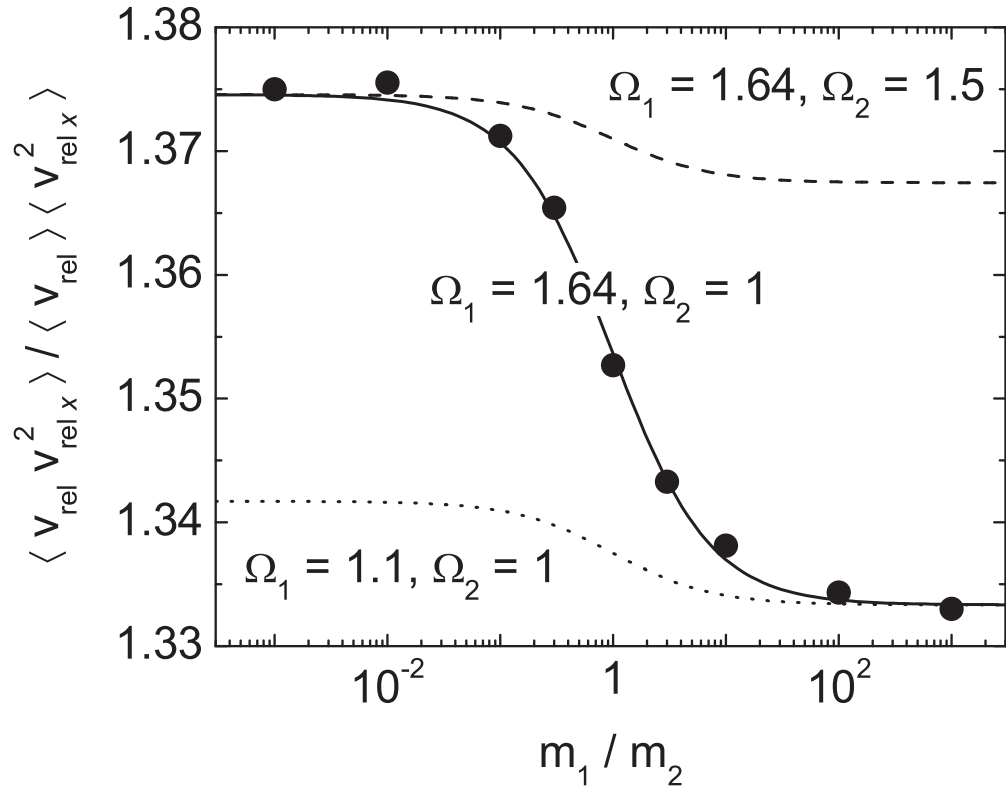


Figure B.1: Effect of energy anisotropies on thermal averages. Shown is the ratio given in Eq.(B.5) as a function of mass ratio  $m_1/m_2$  for different anisotropies. Points are from Monte Carlo integrations, and the solid line is from Eq.(B.3), for the case of  $\Omega_1 = 1.64$  and  $\Omega_2 = 1$ . The dashed and dotted lines are for different anisotropies, as labeled.

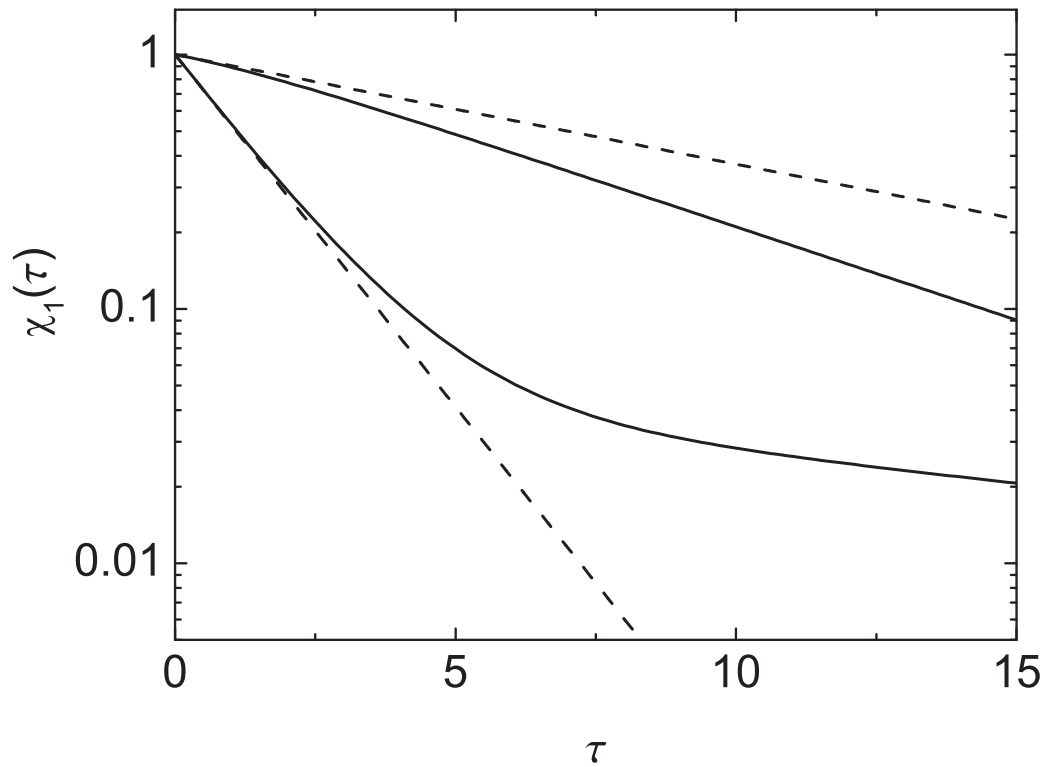


Figure B.2: Fermion relaxation with double exponential decay. Shown is the energy anisotropy of the fermions as a function of time (in units of the mean time  $\tau$  between collisions). The upper (lower) solid curve is the solution to Enskog's equation from Ref. [66], with masses corresponding to a  $^{40}\text{K}$ - $^7\text{Li}$  ( $^6\text{Li}$ - $^{133}\text{Cs}$ ) mixture, and with  $\gamma = 0$ . In each case the dashed line is the exponential decay extrapolated from the small- $\tau$  behavior.

so that we need to solve

$$0 = \int_0^{\infty} d\tau [\chi_1(\tau) - e^{-\tau/\beta_u}] \tau e^{-\tau/\beta_u} \quad . \quad (\text{B.8})$$

Now if we take  $\gamma = 0$  in Eq.(8) of Ref. [66], then

$$\chi_1(\tau) = \frac{(1-\eta)(1-2\eta)e^{-\frac{2}{3}\tau} + \eta e^{-\frac{4}{3}\eta(1-\eta)\tau}}{1-2\eta(1-\eta)} \quad . \quad (\text{B.9})$$

Carrying out the integral leads to the condition

$$\frac{(1-\eta)(1-2\eta)}{(3+2\beta_u)^2} + \frac{\eta}{[3+4\eta\beta_u(1-\eta)]^2} = \frac{1}{36} [1-2\eta(1-\eta)] \quad (\text{B.10})$$

The above polynomial equation is solved numerically with a root finder [134], beginning with an initial guess value of  $\beta_l$  in order to obtain the physical solution.